

¹ **Critical transitions and the fragmenting of global forests**

² **Leonardo A. Saravia^{1 3}, Santiago R. Doyle¹, Benjamin Bond-Lamberty²**

³ 1. Instituto de Ciencias, Universidad Nacional de General Sarmiento, J.M. Gutierrez 1159 (1613), Los
⁴ Polvorines, Buenos Aires, Argentina.

⁵ 2. Pacific Northwest National Laboratory, Joint Global Change Research Institute at the University of
⁶ Maryland–College Park, 5825 University Research Court #3500, College Park, MD 20740, USA

⁷ 3. Corresponding author e-mail: lsaravia@ungs.edu.ar

⁸ **keywords:** Forest fragmentation, early warning signals, percolation, power-laws, MODIS, critical transitions

⁹ **Running title:** Critical fragmentation in global forest

¹⁰ **Abstract**

¹¹ 1. Forests provide critical habitat for many species, essential ecosystem services, and are coupled to
¹² atmospheric dynamics through exchanges of energy, water and gases. One of the most important
¹³ changes produced in the biosphere is the replacement of forest areas with human dominated landscapes.
¹⁴ This usually leads to fragmentation, altering the sizes of patches, the structure and function of the
¹⁵ forest. Here we studied the distribution and dynamics of forest patch sizes at a global level, examining
¹⁶ signals of a critical transition from an unfragmented to a fragmented state.

¹⁷ 2. We used MODIS vegetation continuous field to estimate the forest patches at a global level and de-
¹⁸ fined wide regions of connected forest across continents and big islands. We search for critical phase
¹⁹ transitions, where the system state of the forest changes suddenly at a critical point in time; this
²⁰ implies an abrupt change in connectivity that causes an increased fragmentation level. We studied the
²¹ distribution of forest patch sizes and the dynamics of the largest patch over the last fourteen years,
²² as the conditions that indicate that a region is near a critical fragmentation threshold are related to
²³ patch size distribution and temporal fluctuations of the largest patch.

²⁴ 3. We found some evidence that allows us to analyze fragmentation as a critical transition: most regions
²⁵ followed a power-law distribution over the 14 years. We also found that the Philippines region probably
²⁶ went through a critical transition from a fragmented to an unfragmented state. Only the tropical forest
²⁷ of Africa and South America met the criteria to be near a critical fragmentation threshold.

28 4. This implies that human pressures and climate forcings might trigger undesired effects of fragmentation,
29 such as species loss and degradation of ecosystems services, in these regions. The simple criteria
30 proposed here could be used as an early warning to estimate the distance to a fragmentation threshold
31 in forest around the globe and a predictor of a planetary tipping point.

32 Introduction

33 Forests are one of the most important biomes on earth, providing habitat for a large proportion of species
34 and contributing extensively to global biodiversity (Crowther et al., 2015). In the previous century human
35 activities have influenced global bio-geochemical cycles (Bonan, 2008; Canfield, Glazer, & Falkowski, 2010),
36 with one of the most dramatic changes being the replacement of 40% of Earth's formerly biodiverse land
37 areas with landscapes that contain only a few species of crop plants, domestic animals and humans (J. A.
38 Foley et al., 2011). These local changes have accumulated over time and now constitute a global forcing
39 (Barnosky et al., 2012).

40 Another global scale forcing that is tied to habitat destruction is fragmentation, which is defined as the
41 division of a continuous habitat into separated portions that are smaller and more isolated. Fragmentation
42 produces multiple interwoven effects: reductions of biodiversity between 13% and 75%, decreasing forest
43 biomass, and changes in nutrient cycling (Haddad et al., 2015). The effects of fragmentation are not only
44 important from an ecological point of view but also that of human activities, as ecosystem services are deeply
45 influenced by the level of landscape fragmentation (Mitchell et al., 2015).

46 Ecosystems have complex interactions between species and present feedbacks at different levels of organiza-
47 tion (Gilman, Urban, Tewksbury, Gilchrist, & Holt, 2010), and external forcings can produce abrupt changes
48 from one state to another, called critical transitions (Scheffer et al., 2009). These abrupt state shifts cannot
49 be linearly forecasted from past changes, and are thus difficult to predict and manage (Scheffer et al., 2009).
50 Such 'critical' transitions have been detected mostly at local scales (S. R. Carpenter et al., 2011; Drake &
51 Griffen, 2010), but the accumulation of changes in local communities that overlap geographically can prop-
52 agate and theoretically cause an abrupt change of the entire system at larger scales (Barnosky et al., 2012).
53 Coupled with the existence of global scale forcings, this implies the possibility that a critical transition could
54 occur at a global scale (C. Folke et al., 2011; Rockstrom et al., 2009).

55 Complex systems can experience two general classes of critical transitions (R V Solé, 2011). In so-called first
56 order transitions, a catastrophic regime shift that is mostly irreversible occurs because of the existence of
57 alternative stable states (Scheffer et al., 2001). This class of transitions is suspected to be present in a variety
58 of ecosystems such as lakes, woodlands, coral reefs (Scheffer et al., 2001), semi-arid grasslands (Brandon T.
59 Bestelmeyer et al., 2011), and fish populations (Vasilakopoulos & Marshall, 2015). They can be the result of
60 positive feedback mechanisms (Villa Martín, Bonachela, Levin, & Muñoz, 2015); for example, fires in some
61 forest ecosystems were more likely to occur in previously burned areas than in unburned places (Kitzberger,
62 Aráoz, Gowda, Mermoz, & Morales, 2012).

63 The other class of critical transitions are continuous or second order transitions (Ricard V. Solé & Bascompte,
64 2006). In these cases, there is a narrow region where the system suddenly changes from one domain to another,
65 with the change being continuous and in theory reversible. This kind of transitions were suggested to be
66 present in tropical forest (S. Pueyo et al., 2010), semi-arid mountain ecosystems (McKenzie & Kennedy,
67 2012), tundra shrublands (Naito & Cairns, 2015). The transition happens at a critical point where we can
68 observe a distinctive spatial pattern: scale invariant fractal structures characterized by power law patch
69 distributions (Stauffer & Aharony, 1994).

70 There are several processes that can convert a catastrophic transition to a second order transitions (Villa
71 Martín et al., 2015). These include stochasticity, such as demographic fluctuations, spatial heterogeneities,
72 and/or dispersal limitation. All these components are present in forest around the globe (Filotas et al.,
73 2014; Fung, O'Dwyer, Rahman, Fletcher, & Chisholm, 2016; Seidler & Plotkin, 2006), and thus continuous
74 transitions might be more probable than catastrophic transitions. Moreover there is some evidence of recovery
75 in some systems that supposedly suffered an irreversible transition produced by overgrazing (Brandon T
76 Bestelmeyer, Duniway, James, Burkett, & Havstad, 2013; J. Y. Zhang, Wang, Zhao, Xie, & Zhang, 2005)
77 and desertification (Allington & Valone, 2010).

78 The spatial phenomena observed in continuous critical transitions deal with connectivity, a fundamental
79 property of general systems and ecosystems from forests (Ochoa-Quintero, Gardner, Rosa, de Barros Ferraz,
80 & Sutherland, 2015) to marine ecosystems (Leibold & Norberg, 2004) and the whole biosphere (Lenton &
81 Williams, 2013). When a system goes from a fragmented to a connected state we say that it percolates (R
82 V Solé, 2011). Percolation implies that there is a path of connections that involves the whole system. Thus
83 we can characterize two domains or phases: one dominated by short-range interactions where information
84 cannot spread, and another in which long range interactions are possible and information can spread over
85 the whole area. (The term “information” is used in a broad sense and can represent species dispersal or
86 movement.)

87 Thus, there is a critical “percolation threshold” between the two phases, and the system could be driven close
88 to or beyond this point by an external force; climate change and deforestation are the main forces that could
89 be the drivers of such a phase change in contemporary forests (Bonan, 2008; Haddad et al., 2015). There
90 are several applications of this concept in ecology: species' dispersal strategies are influenced by percolation
91 thresholds in three-dimensional forest structure (Ricard V Solé, Bartumeus, & Gamarra, 2005), and it has
92 been shown that species distributions also have percolation thresholds (He & Hubbell, 2003). This implies
93 that pushing the system below the percolation threshold could produce a biodiversity collapse (J. Bascompte
94 & Solé, 1996; Pardini, Bueno, Gardner, Prado, & Metzger, 2010; Ricard V. Solé, Alonso, & Saldaña, 2004);

95 conversely, being in a connected state (above the threshold) could accelerate the invasion of forest into prairie
96 (Loehle, Li, & Sundell, 1996; Naito & Cairns, 2015).

97 One of the main challenges with systems that can experience critical transitions—of any kind—is that the
98 value of the critical threshold is not known in advance. In addition, because near the critical point a small
99 change can precipitate a state shift of the system, they are difficult to predict. Several methods have been
100 developed to detect if a system is close to the critical point, e.g. a deceleration in recovery from perturbations,
101 or an increase in variance in the spatial or temporal pattern (Boettiger & Hastings, 2012; S. R. Carpenter
102 et al., 2011; Dai, Vorselen, Korolev, & Gore, 2012; Hastings & Wysham, 2010).

103 The existence of a critical transition between two states has been established for forest at global scale in
104 different works (Hirota, Holmgren, Nes, & Scheffer (2011); Verbesselt et al. (2016); Wuyts, Champneys, &
105 House (2017)). It was not probed, but is generally believed, that this constitutes a first order catastrophic
106 transition. The regions where forest can grow are not distributed homogeneously, there are demographic
107 fluctuations in forest growth and disturbances produced by human activities. Due to new theoretical advances
108 (Villa Martín, Bonachela, & Muñoz, 2014; Villa Martín et al., 2015) all these factors imply that if these were
109 first order transitions they will be converted or observed as second order continuous transitions. From this
110 basis we applied indices derived from second order transitions to global forest cover dynamics.

111 In this study, our objective is to look for evidence that forests around the globe are near continuous critical
112 point that represent a fragmentation threshold. We use the framework of percolation to first evaluate if
113 forest patch distribution at a continental scale is described by a power law distribution and then examine
114 the fluctuations of the largest patch. The advantage of using data at a continental scale is that for very
115 large systems the transitions are very sharp (R V Solé, 2011) and thus much easier to detect than at smaller
116 scales, where noise can mask the signals of the transition.

117 Methods

118 Study areas definition

119 We analyzed mainland forests at a continental scale, covering the whole globe, by delimiting land areas with
120 a near-contiguous forest cover, separated with each other by large non-forested areas. Using this criterion,
121 we delimited the following forest regions. In America, three regions were defined: South America temperate
122 forest (SAT), subtropical and tropical forest up to Mexico (SAST), and USA and Canada forest (NA). Europe
123 and North Asia were treated as one region (EUAS). The rest of the delimited regions were South-east Asia

124 (SEAS), Africa (AF), and Australia (OC). We also included in the analysis islands larger than 10^5 km^2 . The
125 mainland region has the number 1 e.g. OC1, and the nearby islands have consecutive numeration (Appendix
126 S4, figure S1-S6).

127 Forest patch distribution

128 We studied forest patch distribution in each defined area from 2000 to 2015 using the MODerate-resolution
129 Imaging Spectroradiometer (MODIS) Vegetation Continuous Fields (VCF) Tree Cover dataset version 051
130 (C. DiMiceli et al., 2015). This dataset is produced at a global level with a 231-m resolution, from 2000
131 onwards on an annual basis. There are several definition of forest based on percent tree cover (J. O. Sexton
132 et al., 2015); we choose a range from 20% to 30% threshold in 5% increments to convert the percentage
133 tree cover to a binary image of forest and non-forest pixels. This range is centered in the definition used by
134 the United Nations' International Geosphere-Biosphere Programme (Belward, 1996), and studies of global
135 fragmentation (Haddad et al., 2015) and includes the range used in other studies of critical transitions (C.
136 Xu et al., 2016). Using this range we try to avoid the errors produced by low discrimination of MODIS VCF
137 between forest and dense herbaceous vegetation at low forest cover and the saturation of MODIS VCF in
138 dense forests (J. O. Sexton et al., 2013). We repeat all the analysis described below for this set of thresholds,
139 except in some specific cases. Patches of contiguous forest were determined in the binary image by grouping
140 connected forest pixels using a neighborhood of 8 forest units (Moore neighborhood).

141 Percolation theory

142 A more in-depth introduction to percolation theory can be found elsewhere (Stauffer & Aharony, 1994) and
143 a review from an ecological point of view is available (B. Oborny, Szabó, & Meszéna, 2007). Here, to explain
144 the basic elements of percolation theory we formulate a simple model: we represent our area of interest by a
145 square lattice and each site of the lattice can be occupied—e.g. by forest—with a probability p . The lattice
146 will be more occupied when p is greater, but the sites are randomly distributed. We are interested in the
147 connection between sites, so we define a neighborhood as the eight adjacent sites surrounding any particular
148 site. The sites that are neighbors of other occupied sites define a patch. When there is a patch that connects
149 the lattice from opposite sides, it is said that the system percolates. When p is increased from low values, a
150 percolating patch suddenly appears at some value of p called the critical point p_c .

151 Thus percolation is characterized by two well defined phases: the unconnected phase when $p < p_c$ (called
152 subcritical in physics), in which species cannot travel far inside the forest, as it is fragmented; in a general

153 sense, information cannot spread. The second is the connected phase when $p > p_c$ (supercritical), species
154 can move inside a forest patch from side to side of the area (lattice), i.e. information can spread over the
155 whole area. Near the critical point several scaling laws arise: the structure of the patch that spans the area
156 is fractal, the size distribution of the patches is power-law, and other quantities also follow power-law scaling
157 (Stauffer & Aharony, 1994).

158 The value of the critical point p_c depends on the geometry of the lattice and on the definition of the
159 neighborhood, but other power-law exponents only depend on the lattice dimension. Close to the critical
160 point, the distribution of patch sizes is:

161 (1) $n_s(p_c) \propto s^{-\alpha}$

162 where $n_s(p)$ is the number of patches of size s . The exponent α does not depend on the details of the
163 model and it is called universal (Stauffer & Aharony, 1994). These scaling laws can be applied for landscape
164 structures that are approximately random, or at least only correlated over short distances (Gastner, Oborny,
165 Zimmermann, & Pruessner, 2009). In physics this is called “isotropic percolation universality class”, and
166 corresponds to an exponent $\alpha = 2.05495$. If we observe that the patch size distribution has another exponent
167 it will not belong to this universality class and some other mechanism should be invoked to explain it.
168 Percolation thresholds can also be generated by models that have some kind of memory (Hinrichsen, 2000;
169 Ódor, 2004): for example, a patch that has been exploited for many years will recover differently than a
170 recently deforested forest patch. In this case, the system could belong to a different universality class, or in
171 some cases there is no universality, in which case the value of α will depend on the parameters and details
172 of the model (Corrado, Cherubini, & Pennetta, 2014).

173 To illustrate these concepts, we conducted simulations with a simple forest model with only two states: forest
174 and non-forest. This type of model is called a “contact process” and was introduced for epidemics (Harris,
175 1974), but has many applications in ecology (Gastner et al., 2009; Ricard V. Solé & Bascompte, 2006). A
176 site with forest can become extinct with probability e , and produce another forest site in a neighborhood
177 with probability c . We use a neighborhood defined by an isotropic power law probability distribution. We
178 defined a single control parameter as $\lambda = c/e$ and ran simulations for the subcritical fragmentation state
179 $\lambda < \lambda_c$, with $\lambda = 2$, near the critical point for $\lambda = 2.5$, and for the supercritical state with $\lambda = 5$ (see
180 supplementary data, gif animations).

181 **Patch size distributions**

182 We fitted the empirical distribution of forest patches calculated for each of the thresholds on the range
183 we previously mentioned. We used maximum likelihood (Clauset, Shalizi, & Newman, 2009; Goldstein,
184 Morris, & Yen, 2004) to fit four distributions: power-law, power-law with exponential cut-off, log-normal,
185 and exponential. We assumed that the patch size distribution is a continuous variable that was discretized
186 by remote sensing data acquisition procedure.

187 We set a minimal patch size (X_{min}) at nine pixels to fit the patch size distributions to avoid artifacts at patch
188 edges due to discretization (Weerman et al., 2012). Besides this hard X_{min} limit we set due to discretization,
189 the power-law distribution needs a lower bound for its scaling behavior. This lower bound is also estimated
190 from the data by maximizing the Kolmogorov-Smirnov (KS) statistic, computed by comparing the empirical
191 and fitted cumulative distribution functions (Clauset et al., 2009). For the log-normal model we constrain
192 the values of the μ parameter to positive values, this parameter controls the mode of the distribution and
193 when is negative most of the probability density of the distribution lies outside the range of the forest patch
194 size data (Limpert, Stahel, & Abbt, 2001).

195 To select the best model we calculated corrected Akaike Information Criteria (AIC_c) and Akaike weights for
196 each model (Burnham & Anderson, 2002). Akaike weights (w_i) are the weight of evidence in favor of model
197 i being the actual best model given that one of the N models must be the best model for that set of N
198 models. Additionally, we computed a likelihood ratio test (Clauset et al., 2009; Vuong, 1989) of the power
199 law model against the other distributions. We calculated bootstrapped 95% confidence intervals (Crawley,
200 2012) for the parameters of the best model; using the bias-corrected and accelerated (BCa) bootstrap (Efron
& Tibshirani, 1994) with 10000 replications.

202 **Largest patch dynamics**

203 The largest patch is the one that connects the highest number of sites in the area. This has been used
204 extensively to indicate fragmentation (R. H. Gardner & Urban, 2007; Ochoa-Quintero et al., 2015). The
205 relation of the size of the largest patch S_{max} to critical transitions has been extensively studied in relation
206 to percolation phenomena (Bazant, 2000; Botet & Ploszajczak, 2004; Stauffer & Aharony, 1994), but seldom
207 used in ecological studies (for an exception see Gastner et al. (2009)). When the system is in a connected
208 state ($p > p_c$) the landscape is almost insensitive to the loss of a small fraction of forest, but close to the
209 critical point a minor loss can have important effects (B. Oborny et al., 2007; Ricard V. Solé & Bascompte,
210 2006), because at this point the largest patch will have a filamentary structure, i.e. extended forest areas

211 will be connected by thin threads. Small losses can thus produce large fluctuations.

212 One way to evaluate the fragmentation of the forest is to calculate the proportion of the largest patch against
213 the total area (Keitt, Urban, & Milne, 1997). The total area of the regions we are considering (Appendix S4,
214 figures S1-S6) may not be the same than the total area that the forest could potentially occupy, thus a more
215 accurate way to evaluate the weight of S_{max} is to use the total forest area, that can be easily calculated
216 summing all the forest pixels. We calculate the proportion of the largest patch for each year, dividing S_{max}
217 by the total forest area of the same year: $RS_{max} = S_{max}/\sum_i S_i$. This has the effect of reducing the S_{max}
218 fluctuations produced due to environmental or climatic changes influences in total forest area. When the
219 proportion RS_{max} is large (more than 60%) the largest patch contains most of the forest so there are fewer
220 small forest patches and the system is probably in a connected phase. Conversely, when it is low (less than
221 20%), the system is probably in a fragmented phase (Saravia & Momo, 2017). As we calculated these largest
222 patch indices for different thresholds, the values of the total forest area and the value of S_{max} are lower as
223 threshold is higher, we expect that the value of RS_{max} will change and probably be lower at high thresholds.
224 To define if a region will be in a connected or unconnected state we used the RS_{max} of the highest threshold
225 (40%) which is more conservative to evaluate the risk of fragmentation and includes the most dense forest
226 area.

227 The RS_{max} is a useful qualitative index that does not tell us if the system is near or far from the critical
228 transition; this can be evaluated using the temporal fluctuations. We calculate the fluctuations around the
229 mean with the absolute values $\Delta S_{max} = S_{max}(t) - \langle S_{max} \rangle$, using the proportions of RS_{max} . To characterize
230 fluctuations we fitted three empirical distributions: power-law, log-normal, and exponential, using the same
231 methods described previously. We expect that large fluctuation near a critical point have heavy tails (log-
232 normal or power-law) and that fluctuations far from a critical point have exponential tails, corresponding to
233 Gaussian processes (Rooij, Nash, Rajaraman, & Holden, 2013). As the data set spans 16 years, it is probable
234 that will do not have enough power to reliably detect which distribution is better (Clauset et al., 2009). To
235 improve this we used the same likelihood ratio test we used previously (Clauset et al., 2009; Vuong, 1989);
236 if the p-value obtained to compare the best distribution against the others we concluded that there is not
237 enough data to decide which is the best model. We generated animated maps showing the fluctuations of
238 the two largest patches at 30% threshold, to aid in the interpretations of the results.

239 A robust way to detect if the system is near a critical transition is to analyze the increase in variance of
240 the density (Benedetti-Cecchi, Tamburello, Maggi, & Bulleri, 2015). It has been demonstrated that the
241 variance increase in density appears when the system is very close to the transition (Corrado et al., 2014),
242 thus practically it does not constitute an early warning indicator. An alternative is to analyze the variance of

243 the fluctuations of the largest patch ΔS_{max} : the maximum is attained at the critical point but a significant
244 increase occurs well before the system reaches the critical point (Corrado et al., 2014; Saravia & Momo,
245 2017). In addition, before the critical fragmentation, the skewness of the distribution of ΔS_{max} should be
246 negative, implying that fluctuations below the average are more frequent. We characterized the increase in
247 the variance using quantile regression: if variance is increasing the slopes of upper or/and lower quartiles
248 should be positive or negative.

249 All statistical analyses were performed using the GNU R version 3.3.0 (R Core Team, 2015), to fit the
250 distributions of patch sizes we used the Python package powerlaw (Alstott, Bullmore, & Plenz, 2014). For
251 the quantile regressions we used the R package quantreg (Koenker, 2016). Image processing was done
252 in MATLAB r2015b (The Mathworks Inc.). The complete source code for image processing and statistical
253 analysis, and the patch size data files are available at figshare <http://dx.doi.org/10.6084/m9.figshare.4263905>.

254 Results

255 The figure 1 shows an example of the distribution of the biggest 200 patches for years 2000 and 2014, this
256 distribution is highly variable, but the biggest patch usually maintains its place. Sometimes the biggest
257 patch breaks and then big fluctuations in its size are observed, as we will analyze below. Smaller patches
258 can merge or break more easily so they enter or leave the list of 200, and this is why there is a color change
259 across years.

260 The power law distribution was selected as the best model in 99% of the cases (Appendix S4, Figure S7).
261 In a small number of cases (1%) the power law with exponential cutoff was selected, but the value of the
262 parameter α was similar by ± 0.03 to the pure power law. Additionally the patch size where the exponential
263 tail begins is very large, thus we used the power law parameters for this cases (See Appendix S4, Figure S2,
264 region EUAS3). In finite-size systems the favored model should be the power law with exponential cutoff,
265 because the power-law tails are truncated to the size of the system (Stauffer & Aharony, 1994). Here the
266 regions are so large that the cutoff is practically not observed.

267 There is only one region that did not follow a power law: Eurasia mainland, which showed a log-normal
268 distribution, representing 7% of the cases. The log-normal and power law are both heavy tailed distributions
269 and difficult to distinguish, but in this case Akaike weights have very high values for log-normal (near 1),
270 meaning that this is the only possible model. In addition, the goodness of fit tests clearly rejected the power
271 law model in all cases for this region (Appendix S4, table S1, region EUAS1). In general the goodness of fit
272 test rejected the power law model in fewer than 10% of cases. In large forest areas like Africa mainland (AF1)

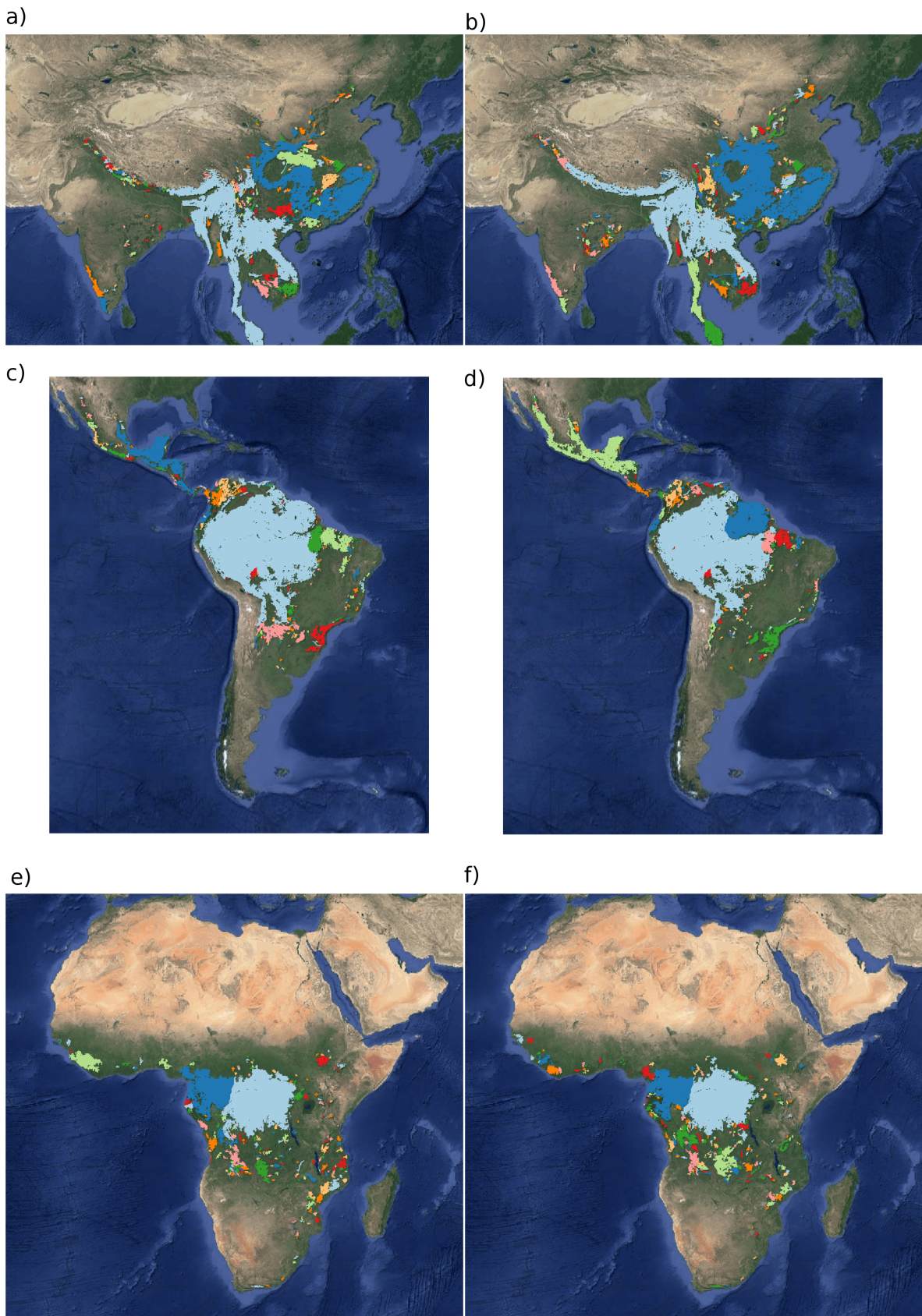


Figure 1: Forest patch distributions for continental regions for the years 2000 and 2014. The images are the 200 biggest patches, showed at a coarse pixel scale of 2.5 Km. The regions are: a) & b) southeast Asia; c) & d) South America subtropical and tropical and e) & f) Africa mainland, for the years 2000 and 2014 respectively. The color palette was chosen to discriminate different patches and do not represent patch size.

273 or South America tropical-subtropical (SAST1), larger deviations are expected and the rejections rates are
274 higher so the proportion is 30% or less (Appendix S4, Table S1).

275 Taking into account the bootstrapped confidence intervals of each power law exponent (α) and the temporal
276 autocorrelation, there were no significant differences between α for the regions with the biggest (greater than
277 10^7 km^2) forest areas (Figure 2 and Appendix S4, Figure S8). There were also no differences between these
278 regions and smaller ones (Appendix S4, Tables S2 & S3), and all the slopes of α were not different from
279 0 (Appendix S4, Table S3). This implies a global average $\alpha = 1.908$, with a bootstrapped 95% confidence
280 interval between 1.898 and 1.920.

281 The proportion of the largest patch relative to total forest area RS_{max} for regions with more than 10^7
282 km^2 of forest is shown in figure 3. South America tropical and subtropical (SAST1) and North America
283 (NA1) have a higher RS_{max} of more than 60%, and other big regions 40% or less. For regions with less
284 total forest area (Appendix S4, figure S9 & Table 1), the Great Britain (EUAS3) has a very low proportion
285 near 1%, while other regions such as New Guinea (OC2) and Malaysia/Kalimantan (OC3) have a very high
286 proportion. SEAS2 (Philippines) is a very interesting case because it seems to be under 30% until the year
287 2005, fluctuates in the range 30-60%, and then stays over 60% (Appendix S4, figure S9).

288 We analyzed the distributions of fluctuations of the largest patch relative to total forest area ΔRS_{max}
289 and the fluctuations of the largest patch ΔS_{max} . The model selection for ΔS_{max} resulted in power law
290 distributions for all regions (Appendix S4, table S6). For ΔRS_{max} instead some regions showed exponential
291 distributions: Eurasia mainland (EUAS1), New Guinea (OC2), Malaysia (OC3), New Zealand (OC6, OC8)
292 and Java (OC7), all others were power laws (Appendix S4, Table S7). The goodness of fit test (GOF) did
293 not reject power laws in any case, but neither did it reject the other models except in a few cases; this was
294 due to the small number of observations. We only considered fluctuations to follow a power law when this
295 distribution was selected for both absolute and relative fluctuations.

296 The animations of the two largest patches (see supplementary data, largest patch gif animations) qualitatively
297 shows the nature of fluctuations and if the state of the forest is connected or not. If the largest patch is
298 always the same patch over time, the forest is probably not fragmented; this happens for regions with RS_{max}
299 of more than 40% such as AF2 (Madagascar), NA1 (North America), and OC3 (Malaysia). In the regions
300 with RS_{max} between 40% and 30% the identity of the largest patch could change or stay the same in time.
301 For OC7 (Java) the largest patch changes and for AF1 (Africa mainland) it stays the same. Only for EUAS1
302 (Eurasia mainland) we observed that the two largest patches are always the same, implying that this region
303 is probably composed of two independent domains and should be divided in further studies. The regions

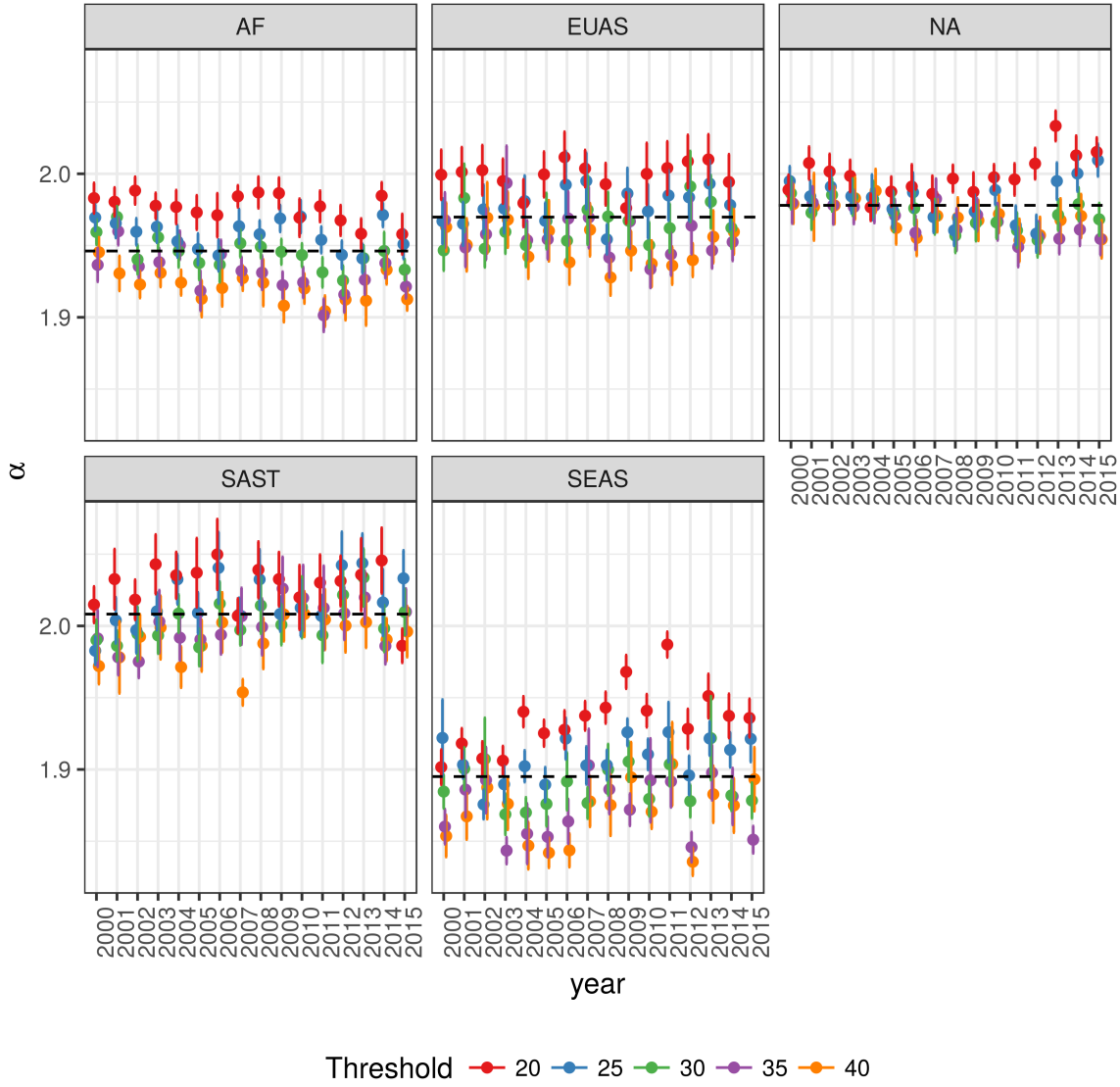


Figure 2: Power law exponents (α) of forest patch distributions for regions with total forest area $> 10^7 \text{ km}^2$. Dashed horizontal lines are the fitted generalized least squares linear model, with 95% confidence interval error bars estimated by bootstrap resampling. The regions are AF1: Africa mainland, EUAS1: Eurasia mainland, NA1: North America mainland, SAST1: South America subtropical and tropical, SEAS1: Southeast Asia mainland. For EUAS1 the best model is log-normal but the exponents are included here for comparison.

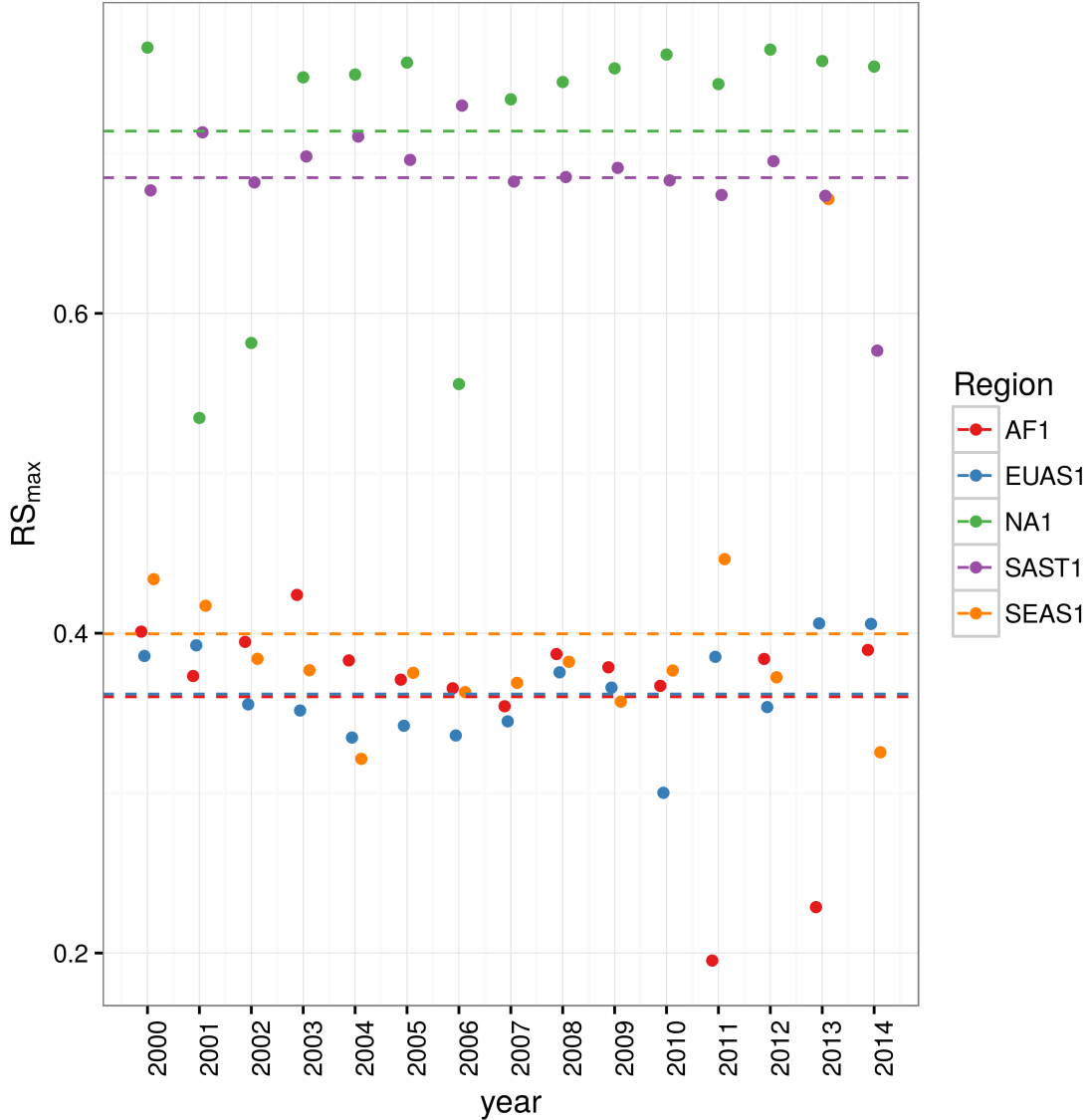


Figure 3: Largest patch proportion relative to total forest area RS_{max} , for regions with total forest area $> 10^7 \text{ km}^2$. Dashed lines are averages across time. The regions are AF1: Africa mainland, EUAS1: Eurasia mainland, NA1: North America mainland, SAST1: South America tropical and subtropical, SEAS1: Southeast Asia mainland.

304 with RS_{max} less than 25%: SAST2 (Cuba) and EUAS3 (Great Britain), the largest patch always changes
305 reflecting their fragmented state. In the case of SEAS2 (Philippines) a transition is observed, with the
306 identity of the largest patch first variable, and then constant after 2010.

307 The results of quantile regressions are identical for ΔRS_{max} and ΔS_{max} (Appendix S4, table S4). Among the
308 biggest regions, Africa (AF1) has upper and lower quantiles with significantly negative slopes, but the lower
309 quantile slope is lower, implying that negative fluctuations and variance are increasing (Figure 4). Eurasia
310 mainland (EUAS1) has only the upper quantile significant with a positive slope, suggesting an increase in the
311 variance. North America mainland (NA1) exhibits a significant lower quantile with positive slope, implying
312 decreasing variance. Finally, for mainland Australia, all quantiles are significant, and the slope of the lower
313 quantiles is greater than the upper ones, showing that variance is decreasing (Appendix S4, figure S10).

314 These results are summarized in Table 1.

315 The conditions that indicate that a region is near a critical fragmentation threshold are that patch size
316 distributions follow a power law; temporal ΔRS_{max} fluctuations follow a power law; variance of ΔRS_{max} is
317 increasing in time; and skewness is negative. All these conditions were true only for Africa mainland (AF1)
318 and South America tropical & subtropical (SAST1).

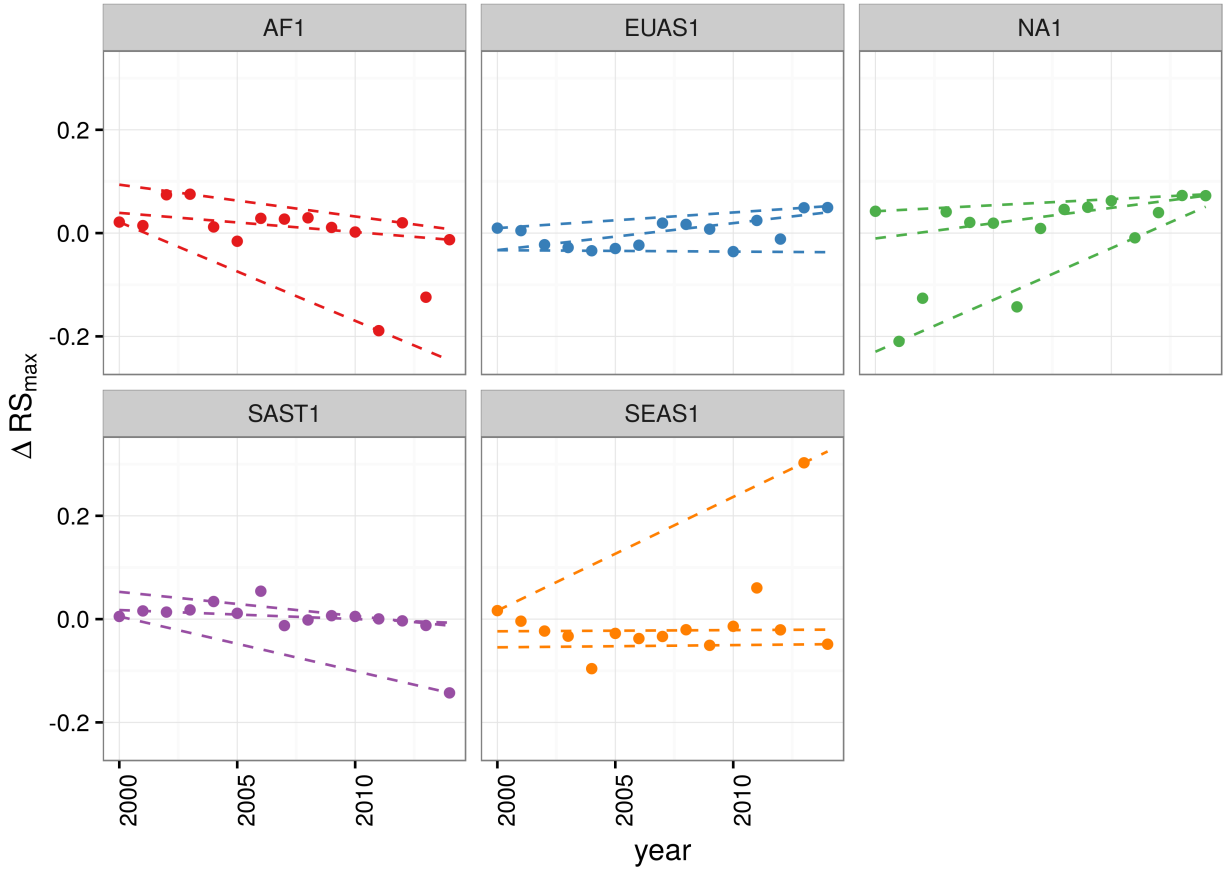


Figure 4: Largest patch fluctuations for regions with total forest area $> 10^7 \text{ km}^2$ across years. The patch sizes are relative to the total forest area of the same year. Dashed lines are 90%, 50% and 10% quantile regressions, to show if fluctuations were increasing. The regions are AF1: Africa mainland, EUAS1: Eurasia mainland, NA1: North America mainland, SAST1: South America tropical and subtropical, SEAS1: Southeast Asia mainland.

Table 1: Regions and indicators of closeness to a critical fragmentation threshold. Where, RS_{max} is the largest patch divided by the total forest area, ΔRS_{max} are the fluctuations of RS_{max} around the mean, skewness was calculated for RS_{max} and the increase or decrease in the variance was estimated using quantile regressions, NS means the results were non-significant. The conditions that determine the closeness to a threshold are: power law distributions in patch sizes and ΔRS_{max} ; increasing variance of ΔRS_{max} and negative skewness.

| Region | Description | Average | Patch Size | | | |
|--------|---|------------|------------|-------------------|----------|----------|
| | | RS_{max} | Distrib | ΔRS_{max} | Distrib. | Skewness |
| AF1 | Africa mainland | 0.36 | Power | Power | -1.8630 | Increase |
| AF2 | Madagascar | 0.65 | Power | Power | -0.2478 | NS |
| EUAS1 | Eurasia, mainland | 0.36 | LogNormal | Exp | 0.4016 | Increase |
| EUAS2 | Japan | 0.94 | Power | Power | 0.0255 | NS |
| EUAS3 | Great Britain | 0.07 | Power | Power | 2.1330 | NS |
| NA1 | North America, mainland | 0.71 | Power | Power | -1.5690 | Decrease |
| NA5 | Newfoundland | 0.87 | Power | Power | -0.7411 | NS |
| OC1 | Australia, Mainland | 0.28 | Power | Power | 0.0685 | Decrease |
| OC2 | New Guinea | 0.97 | Power | Exp | 0.1321 | Decrease |
| OC3 | Malaysia/Kalimantan | 0.97 | Power | Exp | -0.9633 | NS |
| OC4 | Sumatra | 0.92 | Power | Power | 1.3150 | Increase |
| OC5 | Sulawesi | 0.87 | Power | Power | -0.3863 | NS |
| OC6 | New Zealand South Island | 0.76 | Power | Exp | -0.6683 | NS |
| OC7 | Java | 0.38 | Power | Exp | -0.1948 | NS |
| OC8 | New Zealand North Island | 0.75 | Power | Exp | 0.2940 | NS |
| SAST1 | South America, Tropical and subtropical forest up to Mexico | 0.68 | Power | Power | -2.7760 | Increase |
| SAST2 | Cuba | 0.21 | Power | Power | 0.2751 | NS |
| SAT1 | South America, Temperate forest | 0.60 | Power | Power | -1.5070 | Decrease |
| SEAS1 | Southeast Asia, Mainland | 0.40 | Power | Power | 3.0030 | NS |
| SEAS2 | Philippines | 0.54 | Power | Power | 0.3113 | Increase |

319 Discussion

320 We found that the forest patch distribution of most regions of the world followed power laws spanning
 321 seven orders of magnitude. These include tropical rainforest, boreal and temperate forest. Power laws have
 322 previously been found for several kinds of vegetation, but never at global scales as in this study. Interestingly,
 323 Eurasia does not follow a power law, but it is a geographically extended region, consisting of different domains
 324 (as we observed in the largest patch animations, see supplementary data). It is known that the union of two
 325 independent power law distributions produces a lognormal distribution (Rooij et al., 2013). Future studies
 326 should split this region into two or more new regions, and test if the underlying distributions are power laws.
 327 Several mechanisms have been proposed for the emergence of power laws in forest: the first is related self
 328 organized criticality (SOC), when the system is driven by its internal dynamics to a critical state; this has

329 been suggested mainly for fire-driven forests (Hantson, Pueyo, & Chuvieco, 2015; Zinck & Grimm, 2009).
330 Real ecosystems do not seem to meet the requirements of SOC dynamics (McKenzie & Kennedy, 2012; S.
331 Pueyo et al., 2010; Sole, Alonso, & Mckane, 2002). A second possible mechanism, suggested by Pueyo
332 et al. (2010), is isotropic percolation, when a system is near the critical point power law structures arise.
333 This is equivalent to the random forest model that we explained previously, and requires the tuning of an
334 external environmental condition to carry the system to this point. We did not expect forest growth to be a
335 random process at local scales, but it is possible that combinations of factors cancel out to produce seemingly
336 random forest dynamics at large scales. If this is the case the power law exponent should be theoretically
337 near $\alpha = 2.055$; this is close but outside the confidence interval we observed (1.898 - 1.920). The third
338 mechanism suggested as the cause of pervasive power laws in patch size distribution is facilitation (Irvine,
339 Bull, & Keeling, 2016; Manor & Shnerb, 2008): a patch surrounded by forest will have a smaller probability
340 of been deforested or degraded than an isolated patch. We hypothesize that models that include facilitation
341 could explain the patterns observed here. The model of Scanlon et al. (2007) showed an $\alpha = 1.34$ which
342 is also different from our results. Another model but with three states (tree/non-tree/degraded), including
343 local facilitation and grazing, was also used to obtain power laws patch distributions without external tuning,
344 and exhibited deviations from power laws at high grazing pressures (S. Kéfi et al., 2007). The values of the
345 power law exponent α obtained for this model are dependent on the intensity of facilitation, when facilitation
346 is more intense the exponent is higher, but the maximal values they obtained are still lower than the ones
347 we observed. The interesting point is that the value of the exponent is dependent on the parameters, and
348 thus the observed α might be obtained with some parameter combination.

349 It has been suggested that a combination of spatial and temporal indicators could more reliably detect
350 critical transitions (S. Kéfi et al., 2014). In this study, we combined five criteria to detect the closeness to
351 a fragmentation threshold. Two of them were spatial: the forest patch size distribution, and the proportion
352 of the largest patch relative to total forest area (RS_{max}). The other three were the distribution of temporal
353 fluctuations in the largest patch size, the trend in the variance, and the skewness of the fluctuations. Each
354 one of these is not a strong individual predictor, but their combination gives us an increased degree of
355 confidence about the system being close to a critical transition.

356 We found that only the tropical forest of Africa and South America met all five criteria, and thus seem to be
357 near a critical fragmentation threshold. This confirms previous studies that point to these two tropical areas
358 as the most affected by deforestation (M. C. Hansen et al., 2013). Africa seems to be more affected, because
359 the proportion of the largest patch relative to total forest area (RS_{max}) is near 30%, which could indicate
360 that the transition is already started. Moreover, this region was estimated to be potentially bistable, with

361 the possibility to completely transform into a savanna (Staver, Archibald, & Levin, 2011). The main driver
362 of deforestation in this area was smallholder farming.

363 The region of South America tropical forest has a RS_{max} of more than 60%, suggesting that the fragmentation
364 transition is approaching but not yet started. In this region, a striking decline in deforestation rates has
365 been observed in Brasil, which hosts most of the biggest forest patch, but deforestation rates have continued
366 to increase in surrounding countries (Argentina, Paraguay, Bolivia, Colombia, Peru) thus the region is still
367 at a high risk.

368 The monitoring of biggest patches is also important because they contain most of the intact forest landscapes
369 defined by P. Potapov et al. (2008), thus a relatively simple way to evaluate the risk in these areas is to
370 use RS_{max} index. The analysis of RS_{max} reveals that the island of Philippines (SEAS2) seems to be an
371 example of a critical transition from an unconnected to a connected state, the early warning signals can
372 be qualitatively observed: a big fluctuation in a negative direction precedes the transition and then RS_{max}
373 stabilizes over 60% (Figure S9). In addition, there was a total loss of forest cover of 1.9% from year 2000 to
374 2012 (M. C. Hansen et al., 2013) and deforestation rates were not substantially reduced in 1990-2014; this
375 could be the results of an active intervention of the government promoting conservation and rehabilitation
376 of protected areas, ban of logging old-growth forest, reforestation of barren areas, community-based forestry
377 activities, and sustainable forest management in the country's production forest (Lasco et al., 2008). This
378 confirms that the early warning indicators proposed here work in the correct direction.

379 The region of Southeast Asia was also one of the most deforested places in the world, but was not detected
380 as a region near a fragmentation threshold. This is probably due to the forest conservation and restoration
381 programs implemented by the Chinese government, which bans logging in natural forests and monitor illegal
382 harvesting (Viña, McConnell, Yang, Xu, & Liu, 2016). The MODIS dataset does not detect if native forest
383 is replaced by agroindustrial tree plantations like oil palms, that are among the main drivers of deforestation
384 in this area (Malhi, Gardner, Goldsmith, Silman, & Zelazowski, 2014). To improve the estimation of forest
385 patches, data sets as the MODIS cropland probability and others about land use, protected areas, forest
386 type, should be incorporated (M. Hansen et al., 2014; J. O. Sexton et al., 2015).

387 Deforestation and fragmentation are closely related. At low levels of habitat reduction species population
388 will decline proportionally; this can happen even when the habitat fragments retain connectivity. As habi-
389 tat reduction continues, the critical threshold is approached and connectivity will have large fluctuations
390 (Brook, Ellis, Perring, Mackay, & Blomqvist, 2013). This could trigger several negative synergistic effects:
391 populations fluctuations and the possibility of extinctions will rise, increasing patch isolation and decreasing

392 connectivity (Brook et al., 2013). This positive feedback mechanism will be enhanced when the fragmenta-
393 tion threshold is reached, resulting in the loss of most habitat specialist species at a landscape scale (Pardini
394 et al., 2010). Some authors argue that since species have heterogeneous responses to habitat loss and frag-
395 mentation, and biotic dispersal is limited, the importance of thresholds is restricted to local scales or even
396 that its existence is questionable (Brook et al., 2013). Fragmentation is by definition a local process that at
397 some point produces emergent phenomena over the entire landscape, even if the area considered is infinite
398 (B. Oborny, Meszéna, & Szabó, 2005). In addition, after a region's fragmentation threshold connectivity
399 decreases, there is still a large and internally well connected patch that can maintain sensitive species (A. C.
400 Martensen, Ribeiro, Banks-Leite, Prado, & Metzger, 2012). What is the time needed for these large patches
401 to become fragmented, and pose a real danger of extinction to a myriad of sensitive species? If a forest is
402 already in a fragmented state, a second critical transition from forest to non-forest could happen, this was
403 called the desertification transition (Corrado et al., 2014). Considering the actual trends of habitat loss,
404 and studying the dynamics of non-forest patches—instead of the forest patches as we did here—the risk of
405 this kind of transition could be estimated. The simple models proposed previously could also be used to
406 estimate if these thresholds are likely to be continuous and reversible or discontinuous and often irreversible
407 (Weissmann & Shnerb, 2016), and the degree of protection (e.g. using the set-asides strategy Banks-Leite et
408 al. (2014)) than would be necessary to stop this trend.

409 The effectiveness of landscape management is related to the degree of fragmentation, and the criteria to
410 direct reforestation efforts could be focused on regions near a transition (B. Oborny et al., 2007). Regions
411 that are in an unconnected state require large efforts to recover a connected state, but regions that are near
412 a transition could be easily pushed to a connected state; feedbacks due to facilitation mechanisms might
413 help to maintain this state. Crossing the fragmentation critical point in forests could have negative effects
414 on biodiversity and ecosystem services (Haddad et al., 2015), but it could also produce feedback loops at
415 different levels of the biological hierarchy. This means that a critical transition produced at a continental
416 scale could have effects at the level of communities, food webs, populations, phenotypes and genotypes
417 (Barnosky et al., 2012). All these effects interact with climate change, thus there is a potential production of
418 cascading effects that could lead to a global collapse. Therefore, even if critical thresholds are reached only in
419 some forest regions at a continental scale, a cascading effect with global consequences could still be produced,
420 and may contribute to reach a planetary tipping point (Reyer, Rammig, Brouwers, & Langerwisch, 2015).
421 The risk of such event will be higher if the dynamics of separate continental regions are coupled (Lenton &
422 Williams, 2013). Using the time series obtained in this work the coupling of the continental could be further
423 investigated. It has been proposed that to assess the probability of a global scale shift, different small scale

⁴²⁴ ecosystems should be studied in parallel (Barnosky et al., 2012). As forest comprises a major proportion
⁴²⁵ of such ecosystems, we think that the transition of forests could be used as a proxy for all the underling
⁴²⁶ changes and as a successful predictor of a planetary tipping point.

⁴²⁷ **Supporting information**

⁴²⁸ **Appendix**

⁴²⁹ *Table S1:* Proportion of Power law models not rejected by the goodness of fit test at $p \leq 0.05$ level.

⁴³⁰ *Table S2:* Generalized least squares fit by maximizing the restricted log-likelihood.

⁴³¹ *Table S3:* Simultaneous Tests for General Linear Hypotheses of the power law exponent.

⁴³² *Table S4:* Quantile regressions of the proportion of largest patch area vs year.

⁴³³ *Table S5:* Unbiased estimation of skewness for absolute largest patch fluctuations and relative fluctuations.

⁴³⁴ *Table S6:* Model selection using Akaike criterion for largest patch fluctuations in absolute values

⁴³⁵ *Table S7:* Model selection for fluctuation of largest patch in relative to total forest area.

⁴³⁶ *Figure S1:* Regions for Africa (AF), 1 Mainland, 2 Madagascar.

⁴³⁷ *Figure S2:* Regions for Eurasia (EUAS), 1 Mainland, 2 Japan, 3 Great Britain.

⁴³⁸ *Figure S3:* Regions for North America (NA), 1 Mainland, 5 Newfoundland.

⁴³⁹ *Figure S4:* Regions for Australia and islands (OC), 1 Australia mainland; 2 New Guinea; 3 Malaysia/Kalimantan;
⁴⁴⁰ 4 Sumatra; 5 Sulawesi; 6 New Zealand south island; 7 Java; 8 New Zealand north island.

⁴⁴¹ *Figure S5:* Regions for South America, SAST1 Tropical and subtropical forest up to Mexico; SAST2 Cuba;
⁴⁴² SAT1 South America, Temperate forest.

⁴⁴³ *Figure S6:* Regions for Southeast Asia (SEAS), 1 Mainland; 2 Philippines.

⁴⁴⁴ *Figure S7:* Proportion of best models selected for patch size distributions using the Akaike criterion.

⁴⁴⁵ *Figure S8:* Power law exponents for forest patch distributions by year.

⁴⁴⁶ *Figure S9:* Largest patch proportion relative to total forest area RS_{max} , for regions with total forest area
⁴⁴⁷ less than 10^7 km^2 .

⁴⁴⁸ *Figure S10:* Fluctuations of largest patch for regions with total forest area less than 10^7 km^2 . The patch
⁴⁴⁹ sizes are relativized to the total forest area for that year.

450 **Data Accessibility**

451 Csv text file with model fits for patch size distribution, and model selection for all the regions; Gif Animations
452 of a forest model percolation; Gif animations of largest patches; patch size files for all years and regions
453 used here; and all the R and Matlab scripts are available at figshare <http://dx.doi.org/10.6084/m9.figshare.4263905>.

455 **Acknowledgments**

456 LAS and SRD are grateful to the National University of General Sarmiento for financial support. This work
457 was partially supported by a grant from CONICET (PIO 144-20140100035-CO).

458 **References**

- 459 Allington, G. R. H., & Valone, T. J. (2010). Reversal of desertification: The role of physical and chemical
460 soil properties. *Journal of Arid Environments*, 74(8), 973–977. doi:10.1016/j.jaridenv.2009.12.005
- 461 Alstott, J., Bullmore, E., & Plenz, D. (2014). powerlaw: A Python Package for Analysis of Heavy-Tailed
462 Distributions. *PLOS ONE*, 9(1), e85777. Retrieved from <https://doi.org/10.1371/journal.pone.0085777>
- 463 Banks-Leite, C., Pardini, R., Tambosi, L. R., Pearse, W. D., Bueno, A. A., Bruscagin, R. T., ... Metzger,
464 J. P. (2014). Using ecological thresholds to evaluate the costs and benefits of set-asides in a biodiversity
465 hotspot. *Science*, 345(6200), 1041–1045. doi:10.1126/science.1255768
- 466 Barnosky, A. D., Hadly, E. A., Bascompte, J., Berlow, E. L., Brown, J. H., Fortelius, M., ... Smith, A. B.
467 (2012). Approaching a state shift in Earth’s biosphere. *Nature*, 486(7401), 52–58. doi:10.1038/nature11018
- 468 Bascompte, J., & Solé, R. V. (1996). Habitat fragmentation and extinction threholds in spatially explicit
469 models. *Journal of Animal Ecology*, 65(4), 465–473. doi:10.2307/5781
- 470 Bazant, M. Z. (2000). Largest cluster in subcritical percolation. *Physical Review E*, 62(2), 1660–1669.
471 Retrieved from <http://link.aps.org/doi/10.1103/PhysRevE.62.1660>
- 472 Belward, A. S. (1996). *The IGBP-DIS Global 1 Km Land Cover Data Set “DISCover”: Proposal and
473 Implementation Plans : Report of the Land Recover Working Group of IGBP-DIS* (p. 61). IGBP-DIS Office.
474 Retrieved from <https://books.google.com.ar/books?id=qixsNAAACAAJ>
- 475 Benedetti-Cecchi, L., Tamburello, L., Maggi, E., & Bulleri, F. (2015). Experimental Perturbations Mod-

- 476 ify the Performance of Early Warning Indicators of Regime Shift. *Current Biology*, 25(14), 1867–1872.
477 doi:10.1016/j.cub.2015.05.035
- 478 Bestelmeyer, B. T., Duniway, M. C., James, D. K., Burkett, L. M., & Havstad, K. M. (2013). A test of
479 critical thresholds and their indicators in a desertification-prone ecosystem: more resilience than we thought.
480 *Ecology Letters*, 16, 339–345. doi:10.1111/ele.12045
- 481 Bestelmeyer, B. T., Ellison, A. M., Fraser, W. R., Gorman, K. B., Holbrook, S. J., Laney, C. M., ... Sharma,
482 S. (2011). Analysis of abrupt transitions in ecological systems. *Ecosphere*, 2(12), 129. doi:10.1890/ES11-
483 00216.1
- 484 Boettiger, C., & Hastings, A. (2012). Quantifying limits to detection of early warning for critical transitions.
485 *Journal of the Royal Society Interface*, 9(75), 2527–2539. doi:10.1098/rsif.2012.0125
- 486 Bonan, G. B. (2008). Forests and Climate Change: Forcings, Feedbacks, and the Climate Benefits of Forests.
487 *Science*, 320(5882), 1444–1449. doi:10.1126/science.1155121
- 488 Botet, R., & Ploszajczak, M. (2004). Correlations in Finite Systems and Their Universal Scaling Properties.
489 In K. Morawetz (Ed.), *Nonequilibrium physics at short time scales: Formation of correlations* (pp. 445–466).
490 Berlin Heidelberg: Springer-Verlag.
- 491 Brook, B. W., Ellis, E. C., Perring, M. P., Mackay, A. W., & Blomqvist, L. (2013). Does the terrestrial
492 biosphere have planetary tipping points? *Trends in Ecology & Evolution*. doi:10.1016/j.tree.2013.01.016
- 493 Burnham, K., & Anderson, D. R. (2002). *Model selection and multi-model inference: A practical information-
494 theoretic approach* (2nd. ed., p. 512). New York: Springer-Verlag.
- 495 Canfield, D. E., Glazer, A. N., & Falkowski, P. G. (2010). The Evolution and Future of Earth's Nitrogen
496 Cycle. *Science*, 330(6001), 192–196. doi:10.1126/science.1186120
- 497 Carpenter, S. R., Cole, J. J., Pace, M. L., Batt, R., Brock, W. A., Cline, T., ... Weidel, B. (2011).
498 Early Warnings of Regime Shifts: A Whole-Ecosystem Experiment. *Science*, 332(6033), 1079–1082.
499 doi:10.1126/science.1203672
- 500 Clauset, A., Shalizi, C., & Newman, M. (2009). Power-Law Distributions in Empirical Data. *SIAM Review*,
501 51(4), 661–703. doi:10.1137/070710111
- 502 Corrado, R., Cherubini, A. M., & Pennetta, C. (2014). Early warning signals of desertification transitions
503 in semiarid ecosystems. *Physical Review E - Statistical, Nonlinear, and Soft Matter Physics*, 90(6), 62705.

- 504 doi:10.1103/PhysRevE.90.062705
- 505 Crawley, M. J. (2012). *The R Book* (2nd. ed., p. 1076). Hoboken, NJ, USA: Wiley.
- 506 Crowther, T. W., Glick, H. B., Covey, K. R., Bettigole, C., Maynard, D. S., Thomas, S. M., ... Bradford, M.
- 507 A. (2015). Mapping tree density at a global scale. *Nature*, 525(7568), 201–205. doi:10.1038/nature14967
- 508 Dai, L., Vorselen, D., Korolev, K. S., & Gore, J. (2012). Generic Indicators for Loss of Resilience Before a
- 509 Tipping Point Leading to Population Collapse. *Science*, 336(6085), 1175–1177. doi:10.1126/science.1219805
- 510 DiMiceli, C., Carroll, M., Sohlberg, R., Huang, C., Hansen, M., & Townshend, J. (2015). Annual Global Au-
- 511 tomated MODIS Vegetation Continuous Fields (MOD44B) at 250 m Spatial Resolution for Data Years Begin-
- 512 ning Day 65, 2000 - 2014, Collection 051 Percent Tree Cover, University of Maryland, College Park, MD, USA.
- 513 Retrieved from https://lpdaac.usgs.gov/dataset{_\}discovery/modis/modis{_\}products{_\}table/mod44b
- 514 Drake, J. M., & Griffen, B. D. (2010). Early warning signals of extinction in deteriorating environments.
- 515 *Nature*, 467(7314), 456–459. doi:10.1038/nature09389
- 516 Efron, B., & Tibshirani, R. J. (1994). *An Introduction to the Bootstrap* (p. 456). New York: Taylor &
- 517 Francis. Retrieved from <https://books.google.es/books?id=gLlpIUXRntoC>
- 518 Filotas, E., Parrott, L., Burton, P. J., Chazdon, R. L., Coates, K. D., Coll, L., ... Messier, C. (2014). Viewing
- 519 forests through the lens of complex systems science. *Ecosphere*, 5(January), 1–23. doi:10.1890/ES13-00182.1
- 520 Foley, J. A., Ramankutty, N., Brauman, K. A., Cassidy, E. S., Gerber, J. S., Johnston, M., ... Zaks, D. P. M.
- 521 (2011). Solutions for a cultivated planet. *Nature*, 478(7369), 337–342. doi:10.1038/nature10452
- 522 Folke, C., Jansson, Å., Rockström, J., Olsson, P., Carpenter, S. R., Iii, F. S. C., ... Westley, F. (2011).
- 523 Reconnecting to the Biosphere. *AMBIO*, 40(7), 719–738. doi:10.1007/s13280-011-0184-y
- 524 Fung, T., O'Dwyer, J. P., Rahman, K. A., Fletcher, C. D., & Chisholm, R. A. (2016). Reproducing static
- 525 and dynamic biodiversity patterns in tropical forests: the critical role of environmental variance. *Ecology*,
- 526 97(5), 1207–1217. doi:10.1890/15-0984.1
- 527 Gardner, R. H., & Urban, D. L. (2007). Neutral models for testing landscape hypotheses. *Landscape Ecology*,
- 528 22(1), 15–29. doi:10.1007/s10980-006-9011-4
- 529 Gastner, M. T., Oborny, B., Zimmermann, D. K., & Pruessner, G. (2009). Transition from Connected
- 530 to Fragmented Vegetation across an Environmental Gradient: Scaling Laws in Ecotone Geometry. *The*
- 531 *American Naturalist*, 174(1), E23–E39. doi:10.1086/599292
- 532 Gilman, S. E., Urban, M. C., Tewksbury, J., Gilchrist, G. W., & Holt, R. D. (2010). A framework

- 533 for community interactions under climate change. *Trends in Ecology & Evolution*, 25(6), 325–331.
534 doi:10.1016/j.tree.2010.03.002
- 535 Goldstein, M. L., Morris, S. A., & Yen, G. G. (2004). Problems with fitting to the power-law distri-
536 bution. *The European Physical Journal B - Condensed Matter and Complex Systems*, 41(2), 255–258.
537 doi:10.1140/epjb/e2004-00316-5
- 538 Haddad, N. M., Brudvig, L. a., Clobert, J., Davies, K. F., Gonzalez, A., Holt, R. D., ... Townshend, J. R.
539 (2015). Habitat fragmentation and its lasting impact on Earth's ecosystems. *Science Advances*, 1(2), 1–9.
540 doi:10.1126/sciadv.1500052
- 541 Hansen, M. C., Potapov, P. V., Moore, R., Hancher, M., Turubanova, S. A., Tyukavina, A., ... Townshend,
542 J. R. G. (2013). High-Resolution Global Maps of 21st-Century Forest Cover Change. *Science*, 342(6160),
543 850–853. doi:10.1126/science.1244693
- 544 Hansen, M., Potapov, P., Margono, B., Stehman, S., Turubanova, S., & Tyukavina, A. (2014). Response
545 to Comment on “High-resolution global maps of 21st-century forest cover change”. *Science*, 344(6187), 981.
546 doi:10.1126/science.1248817
- 547 Hantson, S., Pueyo, S., & Chuvieco, E. (2015). Global fire size distribution is driven by human impact and
548 climate. *Global Ecology and Biogeography*, 24(1), 77–86. doi:10.1111/geb.12246
- 549 Harris, T. E. (1974). Contact interactions on a lattice. *The Annals of Probability*, 2, 969–988.
- 550 Hastings, A., & Wysham, D. B. (2010). Regime shifts in ecological systems can occur with no warning.
551 *Ecology Letters*, 13(4), 464–472. doi:10.1111/j.1461-0248.2010.01439.x
- 552 He, F., & Hubbell, S. (2003). Percolation Theory for the Distribution and Abundance of Species. *Physical*
553 *Review Letters*, 91(19), 198103. doi:10.1103/PhysRevLett.91.198103
- 554 Hinrichsen, H. (2000). Non-equilibrium critical phenomena and phase transitions into absorbing states.
555 *Advances in Physics*, 49(7), 815–958. doi:10.1080/00018730050198152
- 556 Hirota, M., Holmgren, M., Nes, E. H. V., & Scheffer, M. (2011). Global Resilience of Tropical Forest and
557 Savanna to Critical Transitions. *Science*, 334(6053), 232–235. doi:10.1126/science.1210657
- 558 Irvine, M. A., Bull, J. C., & Keeling, M. J. (2016). Aggregation dynamics explain vegetation patch-size
559 distributions. *Theoretical Population Biology*, 108, 70–74. doi:10.1016/j.tpb.2015.12.001
- 560 Keitt, T. H., Urban, D. L., & Milne, B. T. (1997). Detecting critical scales in fragmented landscapes.

- 561 Conservation Ecology, 1(1), 4. Retrieved from <http://www.ecologyandsociety.org/vol1/iss1/art4/>
- 562 Kéfi, S., Guttal, V., Brock, W. A., Carpenter, S. R., Ellison, A. M., Livina, V. N., ... Dakos, V. (2014).
- 563 Early Warning Signals of Ecological Transitions: Methods for Spatial Patterns. *PLoS ONE*, 9(3), e92097.
- 564 doi:10.1371/journal.pone.0092097
- 565 Kéfi, S., Rietkerk, M., Alados, C. L., Pueyo, Y., Papanastasis, V. P., ElAich, A., & Ruiter, P. C. de.
- 566 (2007). Spatial vegetation patterns and imminent desertification in Mediterranean arid ecosystems. *Nature*,
- 567 449(7159), 213–217. doi:10.1038/nature06111
- 568 Kitzberger, T., Aráoz, E., Gowda, J. H., Mermoz, M., & Morales, J. M. (2012). Decreases in Fire Spread
- 569 Probability with Forest Age Promotes Alternative Community States, Reduced Resilience to Climate Vari-
- 570 ability and Large Fire Regime Shifts. *Ecosystems*, 15(1), 97–112. doi:10.1007/s10021-011-9494-y
- 571 Koenker, R. (2016). quantreg: Quantile Regression. Retrieved from <http://cran.r-project.org/package=quantreg>
- 572
- 573 Lasco, R. D., Pulhin, F. B., Cruz, R. V. O., Pulhin, J. M., Roy, S. S. N., & Sanchez, P. A. J. (2008). Forest
- 574 responses to changing rainfall in the Philippines. In N. Leary, C. Conde, & J. Kulkarni (Eds.), *Climate*
- 575 *change and vulnerability* (pp. 49–66). London: Earthscan. Retrieved from <http://gen.lib.rus.ec/book/index.php?md5=AD313B13E05C9D61A9EC1EE2E73A91FB>
- 576
- 577 Leibold, M. A., & Norberg, J. (2004). Biodiversity in metacommunities: Plankton as complex adaptive
- 578 systems? *Limnology and Oceanography*, 49(4, part 2), 1278–1289. doi:10.4319/lo.2004.49.4_part_2.1278
- 579 Lenton, T. M., & Williams, H. T. P. (2013). On the origin of planetary-scale tipping points. *Trends in*
- 580 *Ecology & Evolution*, 28(7), 380–382. doi:10.1016/j.tree.2013.06.001
- 581 Limpert, E., Stahel, W. A., & Abbt, M. (2001). Log-normal Distributions across the Sciences: Keys and
- 582 CluesOn the charms of statistics, and how mechanical models resembling gambling machines offer a link to
- 583 a handy way to characterize log-normal distributions, which can provide deeper insight into var. *BioScience*,
- 584 51(5), 341–352. Retrieved from [http://dx.doi.org/10.1641/0006-3568\(2001\)051\[0341:LNDATS\]2.0.CO](http://dx.doi.org/10.1641/0006-3568(2001)051[0341:LNDATS]2.0.CO)
- 585 Loehle, C., Li, B.-L., & Sundell, R. C. (1996). Forest spread and phase transitions at forest-prairie ecotones
- 586 in Kansas, U.S.A. *Landscape Ecology*, 11(4), 225–235.
- 587 Malhi, Y., Gardner, T. A., Goldsmith, G. R., Silman, M. R., & Zelazowski, P. (2014). Tropical Forests in
- 588 the Anthropocene. *Annual Review of Environment and Resources*, 39(1), 125–159. doi:10.1146/annurev-

- 589 environ-030713-155141
- 590 Manor, A., & Shnerb, N. M. (2008). Origin of pareto-like spatial distributions in ecosystems. *Physical
591 Review Letters*, 101(26), 268104. doi:10.1103/PhysRevLett.101.268104
- 592 Martensen, A. C., Ribeiro, M. C., Banks-Leite, C., Prado, P. I., & Metzger, J. P. (2012). Associations
593 of Forest Cover, Fragment Area, and Connectivity with Neotropical Understory Bird Species Richness and
594 Abundance. *Conservation Biology*, 26(6), 1100–1111. doi:10.1111/j.1523-1739.2012.01940.x
- 595 McKenzie, D., & Kennedy, M. C. (2012). Power laws reveal phase transitions in landscape con-
596 trols of fire regimes. *Nat Commun*, 3, 726. Retrieved from <http://dx.doi.org/10.1038/ncomms1731>
597 http://www.nature.com/ncomms/journal/v3/n3/supplinfo/ncomms1731{_}S1.html
- 598 Mitchell, M. G. E., Suarez-Castro, A. F., Martinez-Harms, M., Maron, M., McAlpine, C., Gaston, K. J., ...
599 Rhodes, J. R. (2015). Reframing landscape fragmentation's effects on ecosystem services. *Trends in Ecology
600 & Evolution*, 30(4), 190–198. doi:10.1016/j.tree.2015.01.011
- 601 Naito, A. T., & Cairns, D. M. (2015). Patterns of shrub expansion in Alaskan arctic river corridors suggest
602 phase transition. *Ecology and Evolution*, 5(1), 87–101. doi:10.1002/ece3.1341
- 603 Oborny, B., Meszéna, G., & Szabó, G. (2005). Dynamics of Populations on the Verge of Extinction. *Oikos*,
604 109(2), 291–296. Retrieved from <http://www.jstor.org/stable/3548746>
- 605 Oborny, B., Szabó, G., & Meszéna, G. (2007). Survival of species in patchy landscapes: percolation in
606 space and time. In *Scaling biodiversity* (pp. 409–440). Cambridge University Press. Retrieved from <http://dx.doi.org/10.1017/CBO9780511814938.022>
- 608 Ochoa-Quintero, J. M., Gardner, T. A., Rosa, I., de Barros Ferraz, S. F., & Sutherland, W. J. (2015).
609 Thresholds of species loss in Amazonian deforestation frontier landscapes. *Conservation Biology*, 29(2),
610 440–451. doi:10.1111/cobi.12446
- 611 Ódor, G. (2004). Universality classes in nonequilibrium lattice systems. *Reviews of Modern Physics*, 76(3
612 I), 663–724. doi:10.1103/RevModPhys.76.663
- 613 Pardini, R., Bueno, A. de A., Gardner, T. A., Prado, P. I., & Metzger, J. P. (2010). Beyond the Fragmen-
614 tation Threshold Hypothesis: Regime Shifts in Biodiversity Across Fragmented Landscapes. *PLoS ONE*,
615 5(10), e13666. doi:10.1371/journal.pone.0013666
- 616 Potapov, P., Yaroshenko, A., Turubanova, S., Dubinin, M., Laestadius, L., Thies, C., ... Zhuravleva, I. (2008).

- 617 Mapping the world's intact forest landscapes by remote sensing. *Ecology and Society*, 13(2).
- 618 Pueyo, S., de Alencastro Graça, P. M. L., Barbosa, R. I., Cots, R., Cardona, E., & Fearnside, P. M. (2010).
- 619 Testing for criticality in ecosystem dynamics: the case of Amazonian rainforest and savanna fire. *Ecology*
- 620 *Letters*, 13(7), 793–802. doi:10.1111/j.1461-0248.2010.01497.x
- 621 R Core Team. (2015). R: A Language and Environment for Statistical Computing. Vienna, Austria: R
- 622 Foundation for Statistical Computing. Retrieved from <http://www.r-project.org/>
- 623 Reyer, C. P. O., Rammig, A., Brouwers, N., & Langerwisch, F. (2015). Forest resilience, tipping points and
- 624 global change processes. *Journal of Ecology*, 103(1), 1–4. doi:10.1111/1365-2745.12342
- 625 Rockstrom, J., Steffen, W., Noone, K., Persson, A., Chapin, F. S., Lambin, E. F., ... Foley, J. A. (2009). A
- 626 safe operating space for humanity. *Nature*, 461(7263), 472–475. Retrieved from <http://dx.doi.org/10.1038/461472a>
- 627
- 628 Rooij, M. M. J. W. van, Nash, B., Rajaraman, S., & Holden, J. G. (2013). A Fractal Approach to Dynamic
- 629 Inference and Distribution Analysis. *Frontiers in Physiology*, 4(1). doi:10.3389/fphys.2013.00001
- 630 Saravia, L. A., & Momo, F. R. (2017). Biodiversity collapse and early warning indicators in
- 631 a spatial phase transition between neutral and niche communities. *PeerJ PrePrints*, 5, e1589v4.
- 632 doi:10.7287/peerj.preprints.1589v3
- 633 Scanlon, T. M., Caylor, K. K., Levin, S. A., & Rodriguez-iturbe, I. (2007). Positive feedbacks promote
- 634 power-law clustering of Kalahari vegetation. *Nature*, 449(September), 209–212. doi:10.1038/nature06060
- 635 Scheffer, M., Bascompte, J., Brock, W. A., Brovkin, V., Carpenter, S. R., Dakos, V., ... Sugihara, G. (2009).
- 636 Early-warning signals for critical transitions. *Nature*, 461(7260), 53–59. doi:10.1038/nature08227
- 637 Scheffer, M., Walker, B., Carpenter, S., Foley, J. a, Folke, C., & Walker, B. (2001). Catastrophic shifts in
- 638 ecosystems. *Nature*, 413(6856), 591–596. doi:10.1038/35098000
- 639 Seidler, T. G., & Plotkin, J. B. (2006). Seed Dispersal and Spatial Pattern in Tropical Trees. *PLoS Biology*,
- 640 4(11), e344. doi:10.1371/journal.pbio.0040344
- 641 Sexton, J. O., Noojipady, P., Song, X.-P., Feng, M., Song, D.-X., Kim, D.-H., ... Townshend, J. R.
- 642 (2015). Conservation policy and the measurement of forests. *Nature Climate Change*, 6(2), 192–196.
- 643 doi:10.1038/nclimate2816
- 644 Sexton, J. O., Song, X.-P., Feng, M., Noojipady, P., Anand, A., Huang, C., ... Townshend, J. R. (2013).
- 645 Global, 30-m resolution continuous fields of tree cover: Landsat-based rescaling of MODIS vegetation con-

- 646 tinuous fields with lidar-based estimates of error. *International Journal of Digital Earth*, 6(5), 427–448.
 647 doi:10.1080/17538947.2013.786146
- 648 Sole, R. V., Alonso, D., & Mckane, A. (2002). Self-organized instability in complex ecosystems. *Philoso-
 649 sophical Transactions of the Royal Society of London. Series B, Biological Sciences*, 357(May), 667–681.
 650 doi:10.1098/rstb.2001.0992
- 651 Solé, R. V. (2011). *Phase Transitions* (p. 223). Princeton University Press. Retrieved from <https://books.google.com.ar/books?id=8RcLuv-Ll2kC>
- 653 Solé, R. V., & Bascompte, J. (2006). *Self-organization in complex ecosystems* (p. 373). New Jersey, USA.:
 654 Princeton University Press. Retrieved from <http://books.google.com.ar/books?id=v4gpGH6Gv68C>
- 655 Solé, R. V., Alonso, D., & Saldaña, J. (2004). Habitat fragmentation and biodiversity collapse in neutral
 656 communities. *Ecological Complexity*, 1(1), 65–75. doi:10.1016/j.ecocom.2003.12.003
- 657 Solé, R. V., Bartumeus, F., & Gamarra, J. G. P. (2005). Gap percolation in rainforests. *Oikos*, 110(1),
 658 177–185. doi:10.1111/j.0030-1299.2005.13843.x
- 659 Stauffer, D., & Aharony, A. (1994). *Introduction To Percolation Theory* (p. 179). London: Taylor & Francis.
- 660 Staver, A. C., Archibald, S., & Levin, S. A. (2011). The Global Extent and Determinants of Savanna and
 661 Forest as Alternative Biome States. *Science*, 334(6053), 230–232. doi:10.1126/science.1210465
- 662 Vasilakopoulos, P., & Marshall, C. T. (2015). Resilience and tipping points of an exploited fish population
 663 over six decades. *Global Change Biology*, 21(5), 1834–1847. doi:10.1111/gcb.12845
- 664 Verbesselt, J., Umlauf, N., Hirota, M., Holmgren, M., Van Nes, E. H., Herold, M., ... Scheffer, M. (2016). Re-
 665 motely sensed resilience of tropical forests. *Nature Climate Change*, 1(September). doi:10.1038/nclimate3108
- 666 Villa Martín, P., Bonachela, J. A., & Muñoz, M. A. (2014). Quenched disorder forbids discontinuous
 667 transitions in nonequilibrium low-dimensional systems. *Physical Review E*, 89(1), 12145. Retrieved from
 668 <https://link.aps.org/doi/10.1103/PhysRevE.89.012145>
- 669 Villa Martín, P., Bonachela, J. A., Levin, S. A., & Muñoz, M. A. (2015). Eluding catastrophic shifts.
 670 *Proceedings of the National Academy of Sciences*, 112(15), E1828–E1836. doi:10.1073/pnas.1414708112
- 671 Viña, A., McConnell, W. J., Yang, H., Xu, Z., & Liu, J. (2016). Effects of conservation policy on China's
 672 forest recovery. *Science Advances*, 2(3), e1500965. Retrieved from <http://advances.sciencemag.org/content/2/3/e1500965.abstract>
- 674 Vuong, Q. H. (1989). Likelihood Ratio Tests for Model Selection and Non-Nested Hypotheses. *Econometrica*,

- 675 57(2), 307–333. doi:10.2307/1912557
- 676 Weerman, E. J., Van Belzen, J., Rietkerk, M., Temmerman, S., Kéfi, S., Herman, P. M. J., & Koppel, J. V.
677 de. (2012). Changes in diatom patch-size distribution and degradation in a spatially self-organized intertidal
678 mudflat ecosystem. *Ecology*, 93(3), 608–618. doi:10.1890/11-0625.1
- 679 Weissmann, H., & Shnerb, N. M. (2016). Predicting catastrophic shifts. *Journal of Theoretical Biology*, 397,
680 128–134. doi:10.1016/j.jtbi.2016.02.033
- 681 Wuyts, B., Champneys, A. R., & House, J. I. (2017). Amazonian forest-savanna bistability and human
682 impact. *Nature Communications*, 8(May), 15519. doi:10.1038/ncomms15519
- 683 Xu, C., Hantson, S., Holmgren, M., Nes, E. H. van, Staal, A., & Scheffer, M. (2016). Remotely sensed
684 canopy height reveals three pantropical ecosystem states. *Ecology*, 97(9), 2518–2521. doi:10.1002/ecy.1470
- 685 Zhang, J. Y., Wang, Y., Zhao, X., Xie, G., & Zhang, T. (2005). Grassland recovery by protection from
686 grazing in a semi-arid sandy region of northern China. *New Zealand Journal of Agricultural Research*, 48(2),
687 277–284. doi:10.1080/00288233.2005.9513657
- 688 Zinck, R. D., & Grimm, V. (2009). Unifying wildfire models from ecology and statistical physics. *The
689 American Naturalist*, 174(5), E170–85. doi:10.1086/605959